Inorganic Chemistry

ARTICLE

pubs.acs.org/IC

Infrared Spectra of CH_3-MF and Several Fragments Prepared by Methyl Fluoride Reactions with Laser-Ablated Cu, Ag, and Au Atoms

Han-Gook Cho and Lester Andrews*

Department of Chemistry, University of Incheon, 119 Academy-ro, Yonsu-gu, Incheon, 406-772, South Korea

Department of Chemistry, University of Virginia, P.O. Box 400319, Charlottesville, Virginia 22904-4319, United States

Supporting Information

ABSTRACT: Reactions of laser-ablated, excited group 11 metal atoms with CH_3F isotopomers have been carried out, leading to the generation of CH_3-MF and CH_2F-M complexes for Cu, Ag, and Au in addition to smaller complexes for gold. The products in the infrared spectra identified on the basis of their frequencies, isotopic shifts, and correlation with DFT calculated frequencies reveal that M−F insertion by the coinage metals and H atom release readily occur. The relatively low dissociation energies of CH_3-AuF to give several smaller Au complexes are consistent with the observation of these fragments. The C−Au bonds of CF−AuH and CH_2-AuF exhibit considerable π character, and the methylidene CH_2-AuF contains a true double bond. In contrast, the bond orders of CH_2-Au and CH_2-AuH are lower, indicating that F bonded to Au contracts the gold 5d orbitals for better overlap with the carbon 2p orbital for π bonding.

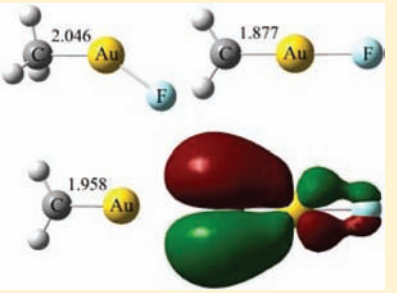

INTRODUCTION

Group 11 metals are distinctive transition-metals with high conductivity and malleability but high electronegativity and catalytic activity as well.[1−3] They are essential not only for surface plasmon spectroscopy but also for coinage, jewelry, and the arts.[4] Their characteristic properties originate from the d^{10} electronic configuration and single valence electron (s^1), leading to borderline elements between the metals and nonmetals. The group 11 metals often behave as Lewis acids with their relatively high electron affinities, unlike other transition metals. Despite the recent increase in research activities, coinage metal complexes with carbon−metal bonds are rare.[1−3]

Alkyl silver and copper have been prepared by reactions of alkyl metals with silver and copper salts at low temperature.[5,6] They are also prepared along with anionic insertion complexes by photodissociation of larger molecules,[7,8] and it has been shown that excited Cu (^2P) plays a key role in the Cu reactions.[7a,9] $CuCH_2$ is observed in the matrix IR spectra from the reaction of Cu with CH_2N_2.[9] More recently, CH_3-MH, CH_3-M, and CH_3-MH^- have been observed in the matrix IR spectra from reactions of laser-ablated group 11 metal atoms with CH_4 and photolysis afterward.[10] The results reveal that coinage metals also readily undergo oxidative C−H bond insertion like other transition metals, and subsequent H release follows. It is interesting that the insertion complexes have higher electron affinities than the coinage metals, which is believed to be the driving force for formation of the rare anionic insertion complex.

Halogen substitution often brings considerable variations to the stabilities and reactivities of the products, mainly due to the general preference for the M−X bond over the M−H bond, and it also helps to understand the chemistry of the small transition-metal complexes.[11] However, small halogen-containing coinage metal complexes with carbon−metal bonds have hardly been reported. Knight et al. have observed CH_3-CuF and HCuF in the matrix ESR spectra from reactions of laser-vaporized Cu atoms with CH_3F,[12] whereas no such studies have been performed for the Ag and Au analogues. Reactivities of group 11 metal cations with methyl fluoride have been examined using mass spectroscopy, and M^+CH_3F complexes for Cu, Ag, and Au and CH_2Au^+ with a carbon−gold double bond have been observed.[13]

In this study, we report the results of group 11 metal atom reactions with CH_3F in excess argon. The products are identified on the basis of isotopic shifts and correlation with DFT calculations. The insertion and fluoromethyl metal complexes for Cu, Ag, and Au and smaller Au methylidene complexes are observed in the matrix IR spectra.

EXPERIMENTAL AND COMPUTATIONAL METHODS

Laser ablated Au, Ag, and Cu atoms were reacted with CH_3F, CD_3F, and $^{13}CH_3F$ (Cambridge Isotope Laboratories, 99%) in excess argon during condensation at 8 K using a closed-cycle refrigerator (Air Products Displex). Reagent gas mixtures are typically 0.5% in argon. These methods have been described in detail in previous publications.[11a,14] The Nd:YAG laser fundamental radiation (1064 nm, 10 Hz repetition rate, 10 ns pulse width) was focused on rotating high purity Au, Ag, and Cu targets using a 5−10 mJ/pulse, and the ablated material was co-deposited with the argon/methyl fluoride samples.[11] After initial reaction, infrared spectra were recorded at a 0.5 cm^{-1} resolution using a

Received: June 28, 2011
Published: September 21, 2011

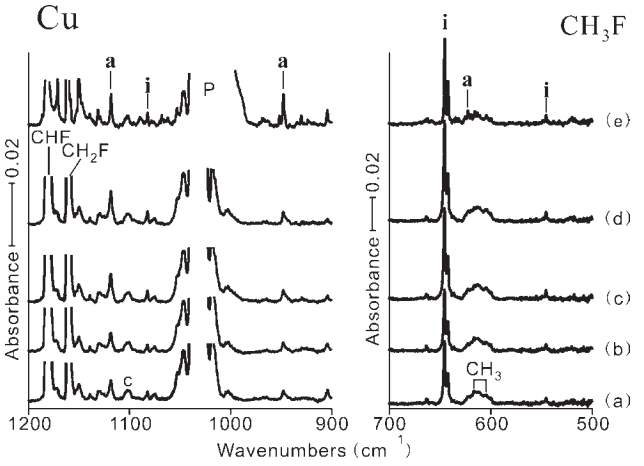

Figure 1. Infrared spectra in the product absorption regions for laser-ablated copper atoms codeposited with CH_3F in excess argon at 8 K and their variation. (a) Cu and CH_3F (0.5% in argon) codeposited for 1 h, (b) as in a after visible (λ > 420 nm) irradiation, (c) as in b after UV (240−380 nm) irradiation, (d) as in c after full arc (λ > 220 nm) photolysis, and (e) as in d after annealing to 28 K. **i** and **a** stand for product absorption groups. P and c denote precursor and common absorptions for different metals, and absorptions from CHF, CH_2F, and CH_3 (fragments of CH_3F) are also indicated.

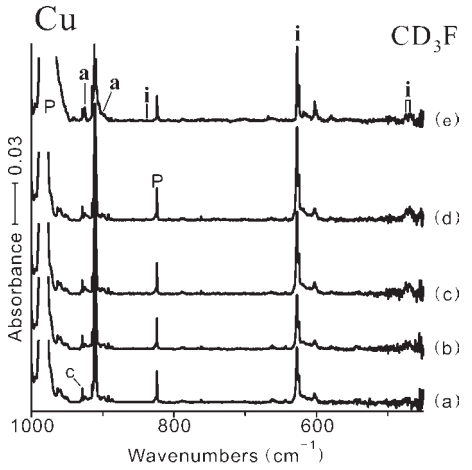

Figure 2. Infrared spectra in the product absorption regions for laser-ablated copper atoms codeposited with CD_3F in excess argon at 8 K and their variation. (a) Cu and CD_3F (0.5% in argon) codeposited for 1 h, (b) as in a after visible (λ > 420 nm) irradiation, (c) as in b after UV (240−380 nm) irradiation, (d) as in c after full arc (λ > 220 nm) photolysis, and (e) as in d after annealing to 28 K. **i** and **a** stand for product absorption groups. P and c denote the precursor and common absorptions for different metals.

Nicolet 550 spectrometer with a Hg−Cd−Te range B detector. Then, samples were irradiated for 20 min periods with a mercury arc street lamp (175 W) with the globe removed using a combination of optical filters, and they were annealed to allow further reagent diffusion.

In order to provide support for the assignment of new experimental frequencies and to correlate with related works,[10,11,15] density functional theory (DFT) calculations were performed using the Gaussian 09 program system;[16] the B3LYP density functional;[17] the 6-311++G-(3df,3pd) basis sets for H, C, F, and Cu;[18] and SDD core potential and basis sets for Au and Ag[19] to provide vibrational frequencies for the

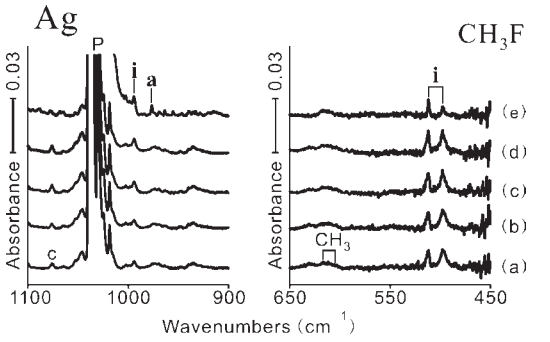

Figure 3. Infrared spectra in the product absorption regions for laser-ablated silver atoms codeposited with CH_3F in excess argon at 8 K and their variation. (a) Ag and CH_3F (0.5% in argon) codeposited for 1 h, (b) as in a after visible (λ > 420 nm) irradiation, (c) as in b after UV (240−380 nm) irradiation, (d) as in c after full arc (λ > 220 nm) photolysis, and (e) as in d after annealing to 28 K. **i** and **a** stand for product absorption groups. P and c denote the precursor and common absorptions for different metals.

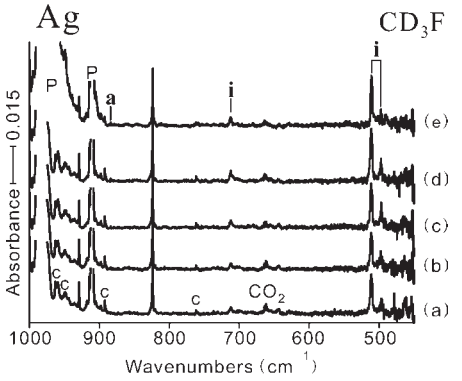

Figure 4. Infrared spectra in the product absorption regions for laser-ablated sliver atoms codeposited with CD_3F in excess argon at 8 K and their variation. (a) Ag and CD_3F (0.5% in argon) codeposited for 1 h, (b) as in a after visible (λ > 420 nm) irradiation, (c) as in b after UV (240−380 nm) irradiation, (d) as in c after full arc (λ > 220 nm) photolysis, and (e) as in d after annealing to 28 K. **i** and **a** stand for product absorption groups. P and c denote the precursor and common absorptions for different metals.

reaction products. Geometries were fully relaxed during optimization, and the optimized geometry was confirmed by vibrational analysis. The BPW91[20] functional was also employed to complement the B3LYP results. The vibrational frequencies are calculated analytically, and zero-point energy is included in the calculation of binding and reaction energies. Previous investigations have shown that DFT calculated harmonic frequencies are usually slightly higher than observed frequencies,[9−13,21] and they provide useful predictions for infrared spectra of new molecules.

RESULTS AND DISCUSSION

The matrix infrared spectra (Figures 1−6 and S1−S3, Supporting Information, and Tables 1−3) from reactions of laser-ablated Cu, Ag, and Au atoms with methyl fluoride isotopomers were investigated, and DFT frequency calculations of the products (Tables S1−S15, Supporting Information) and their structures (Figures 7−9) will be presented in turn. Common absorptions from CH_3F photofragments produced by laser ablation radiation are also shown in the spectra.[11a,22]

dx.doi.org/10.1021/ic2013842 |*Inorg. Chem.* 2011, 50, 10319–10327

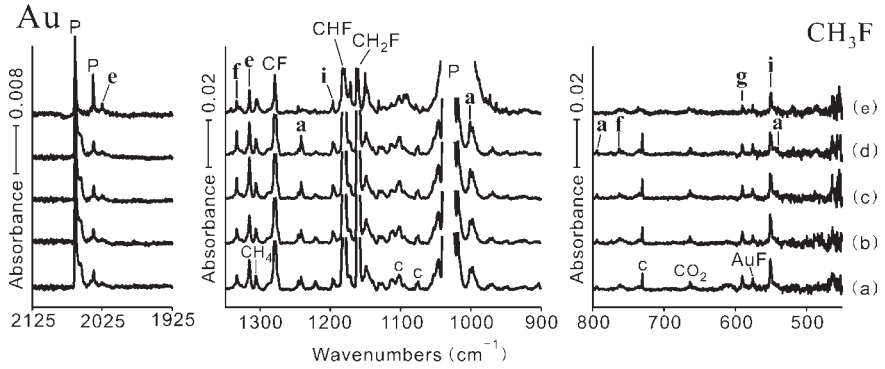

Figure 5. Infrared spectra in the product absorption regions for laser-ablated gold atoms codeposited with CH_3F in excess argon at 8 K and their variation. (a) Au and CH_3F (0.5% in argon) codeposited for 1 h, (b) as in a after visible (λ > 420 nm) irradiation, (c) as in b after UV (240−380 nm) irradiation, (d) as in c after full arc (λ > 220 nm) photolysis, and (e) as in d after annealing to 28 K. **a**, **i**, **e**, **f**, and **g** stand for product absorption groups. P and c denote the precursor and common absorptions for different metals, and the absorptions from CF, CHF, CH_2F, and CH_3 (fragments of CH_3F) are also indicated.

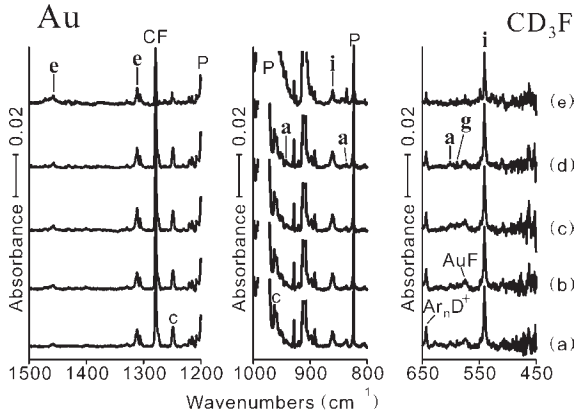

Figure 6. Infrared spectra in the product absorption regions for laser-ablated gold atoms codeposited with CD_3F in excess argon at 8 K and their variation. (a) Au and CD_3F (0.5% in argon) codeposited for 1 h, (b) as in a after visible (λ > 420 nm) irradiation, (c) as in b after UV (240−380 nm) irradiation, (d) as in c after full arc (λ > 220 nm) photolysis, and (e) as in d after annealing to 28 K. **a**, **i**, **e**, **f**, and **g** stand for product absorption groups. P and c denote the precursor and common absorptions for different metals.

Table 1. Frequencies of Product Absorptions Observed from Reactions of Cu with CH_3F Isotopomers in Excess Argon[a]

	CH_3F	CD_3F	$^{13}CH_3F$	description
	1082.3	837.5	1061.0	CH_3−CuF, CH_3 deform
	645.4, 642.0	**627.1**, 624.4	**642.6**, 639.4	CH_3−CuF, Cu−F stretch
i	covered	474	covered	CH_3−CuF, A″ CH_3 rock
	545.4		534.0	CH_3−CuF, A′ CH_3 rock
	1118.5	900.8	1108.5	CH_2F−Cu, CH_2 wag
a	947.7	925.2	927.4	CH_2F−Cu, C−F stretch
	622.5		618.7	CH_2F−Cu, CH_2 rock

[a] All frequencies are in cm^{-1}. Stronger absorptions in a set are bold. Description gives major coordinate.

Cu + CH_3F. Infrared spectra are shown in Figures 1 and 2 and Figure S1 (Supporting Information) for the reaction products of laser ablated Cu atoms codeposited with CH_3F, CD_3F, and $^{13}CH_3F$ in excess argon during condensation at 8 K. Two groups of product absorptions are observed (marked "**i** and **a**" for insertion and fluoromethyl copper complexes). The absorption groups are based on the intensity variations upon photolysis and annealing. The **i** absorptions remain unchanged on visible (λ > 420 nm) irradiation, increase ~50% on UV (240 < λ < 380 nm) irradiation, further increase (~15%) on full arc (λ > 220 nm) irradiation (~65% in total), and gradually decrease on annealing cycles. The **a** absorptions remain unchanged on visible

Table 2. Frequencies of Product Absorptions Observed from Reactions of Ag with CH_3F Isotopomers in Excess Argon[a]

	CH_3F	CD_3F	$^{13}CH_3F$	description
	994.0	711.9	973.3	CH_3−AgF, CH_3 deform
i	512.1, 497.2	**511.1**, 497.3	**511.5**, 497.1	CH_3−AgF, Ag−F stretch
	1145.3	covered	covered	CH_2F−Ag, CH_2 wag
a	963.5	861.0	943.2	CH_2F−Ag, C−F stretch

[a] All frequencies are in cm^{-1}. Description gives major coordinate. Stronger absorptions in a set are bold.

Table 3. Frequencies of Product Absorptions Observed from Reactions of Au with CH_3F Isotopomers in Excess Argon[a]

	CH_3F	CD_3F	$^{13}CH_3F$	description
	1196.5	861.0	1189.1	CH_3−AuF, CH_3 deform
i	550.7	541.2	544.8	CH_3−AuF, Au−F stretch
	1241.5	920.5	1232.8	CH_2F−Au, CH_2 wag
	1001.2	943.5	978.2,	CH_2F−Au, C−F stretch
a	794.3	601.3	790.4	CH_2F−Au, CH_2 rock
	540.4			CH_2F−Au, C−Au stretch
	2025.2	1458.5		CF−AuH, Au−H stretch
e	1315.0	1311.3	1282.5	CF−AuH, C−F stretch
	1332.2	covered	1325.9	CH_2−Au, CH_2 scissor
f	762.9	579.0	758.1	CH_2−Au, CH_2 rock
g	590.1	589.1	589.6	CH_2−AuF, Au−F stretch[b]
AuF	575	575	575	Ar−AuF, Au−F stretch[c]

[a] All frequencies are in cm^{-1}. Description gives major coordinate. [b] Probable assignment. [c] Ref 24.

dx.doi.org/10.1021/ic2013842 |*Inorg. Chem.* 2011, 50, 10319–10327

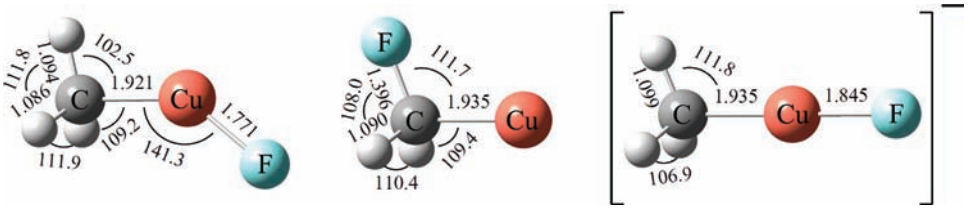

Figure 7. The B3LYP structures of the identified Cu products with the 6-311++G(3df,3pd) basis sets for H, C, F, and Cu. Bond distances and angles are in Ångstroms and degrees. The identified insertion complex and fluoromethyl copper have C_s structures, whereas the unidentified anionic insertion complex (CH_3-CuF^-) possesses a near C_{3v} structure.

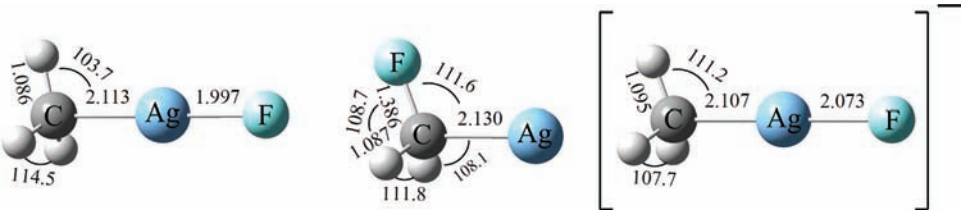

Figure 8. The B3LYP structures of the Ag products with the 6-311++G(3df,3pd) basis sets for H, C, and F and the SDD pseudo-potential and basis set for Ag. Bond distances and angles are in Ångstroms and degrees. The insertion complex (CH_3-AgF) and CH_2F-Ag are identified in the matrix IR spectra (see text). CH_3-AgF carries an unusual linear C−Ag−F moiety, whereas CH_3-AgF^- has a near C_{3v} structure.

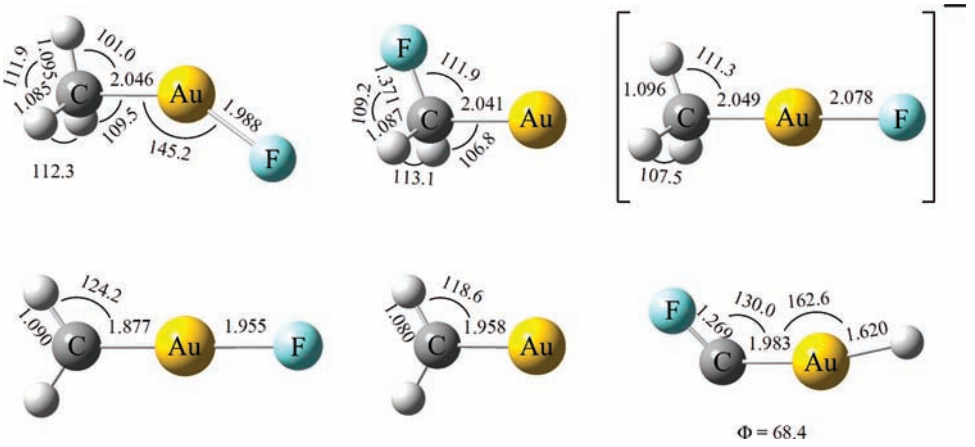

Figure 9. The B3LYP structures of the Au products with the 6-311++G(3df,3pd) basis sets for H, C, and F and the SDD pseudo-potential and basis set for Au. Bond distances and angles are in Ångstroms and degrees. The gold insertion complex and its fragments (CH_3-AuF, CH_2F-Au, CF−AuH, CH_2-Au, and CH_2-AuF) are observed, whereas the anionic insertion complex (CH_3-AuF^-) is not. CF−AuH has a C_1 structure (the dihedral angle is shown). CH_3-AuF^- has a near C_{3v} structure, while the other products carry C_s structures.

irradiation, increase ~50% on UV irradiation, slightly decrease on full arc photolysis, sharpen in the early stages of annealing, and decrease later. The observed product absorptions are summarized in Table 1. In the Cu−H stretching region (1950−1750 cm^{-1}), no product absorption is observed other than the weak CuH absorption at 1878.5 cm^{-1}.[7a,23]

The predominantly strong **i** absorption is observed at 645.4 cm^{-1}, and D and ^{13}C substitution shift it to 627.1 and 642.6 cm^{-1} (H/D and 12/13 ratios of 1.029 and 1.004). It is compared with the CuF, CuF_2, and CuF_3 frequencies of 615.9, 743.1, and 762.3 cm^{-1}.[24] On the basis of its frequency, high absorption intensity, and relatively small isotopic shifts, it is assigned to the Cu−F stretching mode of the C−F bond insertion product (CH_3-CuF) in line with the previous results of transition-metal reactions with CH_3F. The second strong CH_3 deformation absorption is observed at 1082.3 cm^{-1} along with its D and ^{13}C counterparts at 837.5 and 1061.0 cm^{-1} (H/D and 12/13 ratios of 1.292 and 1.020). The third strong A″ CH_3 rocking mode is apparently overlapped by the broad CH_3 absorption (615−602 cm^{-1}), while its D counterpart is observed at 474 cm^{-1}. The weak A′ CH_3 rocking mode is observed at 545.4 cm^{-1} with its ^{13}C counterpart at 534.0 cm^{-1}.

While the observed absorptions show reasonable agreement with the predicted values (Table S1, Supporting Information) using the all-electron basis set for Cu. However, the DFT methods underestimate the Cu−F frequency. For comparison, B3LYP calculation using the SDD pseudopotential for Cu underestimated the Cu−F stretch 5 cm^{-1} more and overestimated the CH_3 deformation 28 cm^{-1} more and the CH_3 rock 17 cm^{-1} more than the all-electron set. Evidently, CH_3-CuF is the only

insertion product more stable than the reactants. The CH_3-CuF molecule in its doublet ground state is 69 kJ/mol more stable than $Cu(^2S) + CH_3F$, whereas the quartet and sextet states are 272 and 975 kJ/mol higher in energy. Another plausible insertion product, CH_2F-CuH, is 83 kJ/mol higher than the reactants, and attempts at geometry optimization for CH_2-CuHF and $CH-CuH_2F$ all finish with the structure of CH_3-CuF, reflecting that the energetically higher Cu methylidene is not a meaningful energy minimum.

Generation of CH_3-CuF from the reaction of Cu with CH_3F and the previously observed CH_3-CuH analog[10] reveal that copper is an effective C−H and C−X bond insertion agent in reactions with small alkanes and halomethanes like other transition metals including lanthanides and actinides. However, subsequent H migration from C to Cu to produce a stable Cu methylidene does not occur, showing that the Cu compounds with more than two bonds to Cu are far less favored.

The strong **a** absorption is observed at 947.7 cm^{-1} along with its D and ^{13}C counterparts at 925.2 and 927.4 cm^{-1}, and on the basis of its frequency and relatively small D and large ^{13}C isotopic shifts, it is most probably the C−F stretching mode of another Cu product. In line with the previously reported alkyl Cu,[6−10] the **a** absorptions are designated to fluoromethyl Cu (CH_2F-Cu), which correlate well with the predicted frequency of 981.3 cm^{-1} and D and ^{13}C isotopic shifts of 23.4 and 22.5 cm^{-1}. The **a** absorption at 1118.5 cm^{-1} is designated to the CH_2 wagging mode with its D and ^{13}C counterparts at 900.8 and 1108.5 cm^{-1}. Another **a** absorption at 622.5 cm^{-1} on the edge of the broad CH_3 absorption carries its ^{13}C counterparts at 618.7 cm^{-1} and is assigned to the CH_2 rocking mode. The **a** absorptions in the CD_3F spectra are weaker, probably due to the lower dissociation rate of the deuterated species.

CH_2F-Cu is 184 kJ/mol more stable than $Cu(^2S) + CH_2F$, whereas CH_2-CuF and $CHF-CuH$ are only 138 and 20 kJ/mol more stable. CH_2-CuF and $CHF-CuH$ would show strong Cu−F and C−F stretching bands at about 570 and 1170 cm^{-1}, which are not observed in this study. Observation of CH_3-Cu[7,10] and CH_2F-Cu from copper reactions with CH_4 and CH_3F reflect the easy release of H in favor of the single valence closed-shell Cu complex. Unlike the previous study of coinage metal reactions with methane,[10] no anionic species (CH_3-MF^-) is observed in this study. HCuF, reported by Knight et al. from the more sensitive ESR spectrum,[12] which would show a strong Cu−H absorption near 1930 cm^{-1}, is also not observed.

Ag + CH_3F. Figures 3 and 4 and Figure S2 (Supporting Information) show the product absorptions marked "**i**" and "**a**" from Ag reactions with CH_3F isotopomers. The **i** absorptions increase 20 and 40% on UV and full arc photolysis and decrease on annealing. The **a** absorptions also increase on UV and full arc photolysis and sharpen on the early stage of annealing. No product absorption is observed in the Ag−H stretching region (1700−1500 cm^{-1}).

The strongest **i** absorption is observed at 512.1 cm^{-1} (with matrix site absorption at 497.2), and it shifts to 511.1 and 511.5 cm^{-1} (with matrix site absorptions at 497.3 and 497.1 cm^{-1}) on deuteration and ^{13}C substitution. It is compared with the AgF, AgF_2, and AgF_3 frequencies of 497.3, 621.5, and 661.9 cm^{-1}.[24] Its frequency, high intensity, and small isotopic shifts lead to an assignment to the Ag−F stretching mode of CH_3-AgF. The observed frequency and D and ^{13}C isotopic shifts are also in good agreement with the predicted values of 528.3 and 3.1 and 0.8 cm^{-1}. The CH_3 deformation absorption is observed at 994.0 cm^{-1} along with its D and ^{13}C counterparts at 712.0 and 973.3 cm^{-1} (H/D and 12/13 ratios of 1.396 and 1.021), showing a reasonable correlation with the predicted frequency of 1008.2 cm^{-1} and D and ^{13}C isotopic shifts of 250.4 and 9.7 cm^{-1}.

CH_3-AgF is 60 kJ/mol higher than the reactants ($Ag(^2S) + CH_3F$), whereas CH_2F-AgH is 150 kJ/mol higher than the reactants, and optimization of CH_2-AgHF again leads to the structure of CH_3-AgF. While CH_3-Ag is observed, CH_3-AgH is unidentified in the previous study for Ag reactions with CH_4, probably due to its high energy (161 kJ/mol higher than $Ag(^2S) + CH_4$).[10] In fact, the insertion reaction most probably occurs with $Ag(^2P)$,[25] which is 353 kJ/mol higher than the ground state ($Ag(^2S)$) and makes the C−F insertion reaction 293 kJ/mol exothermic.

The **a** absorption at 963.5 cm^{-1} is accompanied by the ^{13}C counterpart at 943.2 cm^{-1} and the weak D counterpart at 861.0 cm^{-1}, and it is designated to the C−F stretching mode of CH_2F-Au, in line with the Cu case. The weak **a** absorption at 1145.3 cm^{-1} is assigned to the CH_2 wagging mode without observation of the isotopic counterparts. CH_2F-Ag is again the most stable among the plausible products; CH_2F-Ag, CH_2-AgF, and $CHF-AgH$ are −136, 3, and 63 kJ/mol higher than $Ag(^2S) + CH_2F$.

Au + CH_3F. Figures 5 and 6 and Figure S3 (Supporting Information) show the reaction product spectra from Au atoms codeposited with CH_3F isotopomers in excess argon during condensation at 8 K. The Au + CH_3F spectra are more complicated with product absorptions marked **i**, **a**, **e**, **f**, and **g** depending on the intensity variation in the process of photolysis and annealing. The weak 575 cm^{-1} band is in agreement with a recent observation for AuF in solid argon, which is in fact the Ar−AuF species.[24] The latter species has been observed using microwave spectroscopy and characterized using theoretical calculations.[26,27]

The **i** absorptions slightly decrease during photolysis, whereas the **a** absorptions increase ∼30% on UV irradiation and another ∼30% on full arc photolysis. The broad **e** absorptions slightly decrease on visible irradiation, increase ∼50% on UV irradiation, and decrease ∼30% on full arc photolysis. The sharp **f** absorptions slightly increase on visible irradiation, double on UV irradiation, and further increase ∼20% (∼230% increase in total). The **g** absorption decreases stepwise to ∼80% of its original intensity during the process of photolysis.

The strong **i** absorption at 550.7 cm^{-1} has its D counterpart at 541.2 cm^{-1} and its ^{13}C counterpart at 544.8 cm^{-1}. It is compared with the AuF and AuF_2 frequencies of 575.1 and 640.1 cm^{-1}.[24] On the basis of its frequency, strong absorption intensity, and small isotopic shifts and in line with the Cu and Ag cases, we assign the 550.7 cm^{-1} band to the Au−F stretching mode of CH_3-AuF. This Au−F stretching frequency is lower than the corresponding Cu−F stretching frequency of 645.4 cm^{-1}, but it is higher than the Ag−F stretching frequency of 512.1 cm^{-1}, which is a good example of relativistic contraction.[28] Its CH_3 deformation mode is observed at 1196.5 cm^{-1} with the D and ^{13}C counterparts at 861.0 and 1189.1 cm^{-1}.

It is also noticeable that, similar to the Cu case, the Au−F stretching frequency is considerably underestimated by the B3LYP calculation (underestimation of 26.8 and 53.4 cm^{-1} for the Cu and Au insertion complexes). One problem here is that the Au−F and C−Au stretching modes are mixed with the C−H deformation mode, and the calculation is not adequate to sort this out. The CCSD method[16,29] predicts these frequencies at 1221, 561, and 540 cm^{-1}, which shows better agreement with experimental results.

Frequency underestimations using DFT methods for small coinage metal complexes are apparently common, as shown previously.[10] The M−H stretching frequencies are underestimated by 6.8, 7.5, and 25.5 cm^{-1} for the Cu, Ag, and Au CH_3-MH^- anionic insertion complexes and 11.3 cm^{-1} underestimated for CH_3-CuH. The CH_3 deformation frequency of CH_3-Cu is also 82.1 cm^{-1} underestimated.

CH_3-AuF is 34 kJ/mol higher than Au(^{2}S) + CH_3F, whereas previously observed CH_3-AuH is 80 kJ/mol higher than Au(^{2}S) + CH_4.[10] The C−H insertion product CH_2F-AuH is 72 kJ/mol higher than the reactants and not observed on the basis of its computed frequencies, while CH_2-AuHF is not a meaningful energy minimum. Parallel to the Cu and Ag cases, the Au insertion into the C−F bond reaction probably proceeds with Au(^{2}P) produced in the ablation process, which is 446 kJ/mol higher in energy than Au(^{2}S);[25] therefore, the insertion product is 412 kJ/mol lower in energy than Au(^{2}P) + CH_3F reagents.

The strongest **a** absorption is observed at 1001.2 cm^{-1}, and deuteration shifts it to 943.5 cm^{-1} and ^{13}C substitution to 978.2 cm^{-1}. On the basis of its frequency and small isotopic shifts and in line with the Cu and Ag cases, we assign it to the C−F stretching mode of fluoromethyl gold (CH_2F-Au). Its second strong CH_2 wagging absorption is observed at 1241.5 cm^{-1} along with D and ^{13}C counterparts at 920.5 and 1232.8 cm^{-1}. Its CH_2 rocking and C−Au stretching modes are observed at 794.3 and 540.4 cm^{-1}. The **a** absorptions with their frequencies and relative intensities in reasonable correlation with the predicted values (Table S8, Supporting Information) substantiate the generation of CH_2F-Au in the preference for the single valence closed-shell compound.

The strong **e** absorption at 1315.0 cm^{-1} is accompanied by its D and ^{13}C counterparts at 1311.3 and 1282.5 cm^{-1} (H/D and 12/13 ratios of 1.002 and 1.026). While its small D and considerable ^{13}C shifts are indicative of a C−F stretching mode, its frequency is relatively high. Unusually high C−X stretching frequencies have been observed from the small transition-metal methylidyne complexes ($XC\equiv MX_3$), for example, 1551.2 cm^{-1} for $FC\equiv OsCl_3$.[30] Due to its linear X−C−M moiety, the C−X stretching mode is essentially an X−C−M antisymmetric stretching mode, leading to the distinctively high C−X stretching frequency.

Among the plausible Au insertion complexes and their fragments, only CF−AuH shows an appropriate computed C−F stretching frequency. Much lower C−F stretching frequencies are predicted for all other plausible products, for example, 1083.3 and 1222.3 cm^{-1} for CH_2F-AuH and CHF−AuH. On the basis of the excellent correlation of the observed frequency of 1315.0 cm^{-1} and its D and ^{13}C shifts of 3.7 and 32.5 cm^{-1} with the B3LYP frequency of 1327.0 and the D and ^{13}C shifts of 4.0 and 32.7 cm^{-1}, we assign it to the C−F stretching mode of CF−AuH. Although CF−AuH is nonlinear, as shown in Figure 9 (<FCAu = 130.0), the C−F stretching mode is still substantially mixed with the C−Au stretching mode, leading to the relatively high C−F stretching frequency, although it is not as high as those of the small transition-metal methylidynes.[30] The weak **e** absorption at 2025.2 cm^{-1} with its D counterpart at 1458.5 cm^{-1} is designated to the Au−H stretching mode.

A sharp strong **f** absorption is observed at 1332.2 cm^{-1} with its ^{13}C counterpart at 1325.9 cm^{-1} (12/13 ratio of 1.005), and its frequency and small ^{13}C shift suggest a CH_2 bending mode. Computation results show that only methylidene gold (CH_2-Au) among the plausible products has a strong CH_2 scissoring band in this frequency region. The D counterpart is most probably covered by precursor absorption at ~1000 cm^{-1} (Table S10, Supporting Information). Its second strong CH_2 rocking absorption is observed at 762.9 cm^{-1} along with its ^{13}C counterpart at 758.1 cm^{-1}. However, CH_2-Au was not observed in our recent gold−methane investigation,[10] but it may be compared with CH_2-Cu from the reaction of Cu with CH_2N_2 and subsequent photodissociation.[9] Li and Armentrout reported observation of CH_2-Au^+ by ion beam tandem mass spectrometry,[13] but based on the absence of its strongest IR band near 1029 cm^{-1}, this cation is not observed here.

In addition, a relatively weaker product absorption marked "**g**" at 590.1 cm^{-1} shows small D and ^{13}C isotopic shifts to 589.1 and 589.6 cm^{-1} (Table 3). They are probably due to the Au−F stretching modes of CH_2-AuF, which is computed to have a strong Au−F stretching band in this frequency region with isotopic shifts within 0.2 cm^{-1} of the observed shifts, and other bands are too weak to observe, as shown in Table S11 (Supporting Information). This Au−F stretching modes is calculated to be 11−22 cm^{-1} lower (B3LYP and BPW91) than observed, a smaller underestimation than described above for CH_3-AuF.

CH_2F-Au, CH_2-AuF, and CHF−AuH are 198, 101, and 53 kJ/mol more stable than Au(^{2}S) + CH_2F, consistent with the strong **a** and weaker **g** absorptions. The latter CHF−AuH is not observed in this study, as CH_2F-Au + H is still 208 kJ/mol higher than Au(^{2}S) + CH_3F. The CF−AuH species is 149 kJ/mol more stable than Au(^{2}S) + CHF but 276 kJ/mol higher energy than Au(^{2}S) + CH_3F. Although CHF−Au is predicted to be 110 kJ/mol more stable than CF−AuH, it is not observed in this study. One possibility is that the strongest C−F stretching absorption expected near 1110 cm^{-1} is covered in this congested region. CH_2-Au is 258 kJ/mol more stable than Au(^{2}S) + CH_2, while CH_2-Au + HF is only 90 kJ/mol higher than Au(^{2}S) + CH_3F. The latter relatively small dissociation energy to CH_2-Au + HF is consistent with the strong **f** absorptions in the original spectra and their dramatic increase during photolysis.

Reactions. The strong **i** absorptions in the original deposition spectra suggest that CH_3-MF is first produced via C−F insertion of CH_3F by M* (excited), similar to the previously studied transition-metal systems.[11,30] The earlier photochemical reactions of Cu with methane showed that ^{2}P (365 kJ/mol higher than ^{2}S)[25] Cu atoms are involved in the insertion reaction.[7a] Similar excitation in the laser ablation process and subsequent UV irradiation can provide the required energy for C−F bond insertion by group 11 metals. The absorptions of the previously studied methyl coinage metal hydrides (CH_3-MH) nearly disappear on visible irradiation, while the CH_3-M absorptions increase, a sign of photodissociation of the insertion complex to the methyl metal species.[10] CH_3-MF, which does not show a similar dramatic decrease in the absorption intensities, is evidently more stable during photolysis. Instead, they increase 60 and 65% in the Cu and Ag systems and slightly decrease in the Au case.

$$M^*(^2P) + CH_3F \rightarrow CH_3-MF^* \rightarrow CH_3-MF \quad (1a)$$

$$M^*(^2P) + CH_3F \rightarrow CH_2F-MH^* \rightarrow CH_2F-M + H \quad (1b)$$

The CH_2F-M products are probably made by C−H insertion to form the higher energy CH_2F-MH species, which relax by

dx.doi.org/10.1021/ic2013842 |Inorg. Chem. 2011, 50, 10319–10327

eliminating H. However, in our Pt experiments, CH_2F-PtH was observed.[11d]

The fragments of CH_3F (CH_3, CH_2F, CHF, and CF) are produced and trapped in these experiments from laser plume photodissociation of methyl fluoride.[31] Thus, the reaction medium contains not only coinage metal atoms and CH_3F but the CH_3F fragments as well, and reactions of these components could produce the identified products, particularly on annealing.

$$CH_2F + M \rightarrow CH_2F-M, CH_2-MF \quad (2a)$$

$$CHF + M \rightarrow CF-MH, CHF-M \quad (2b)$$

$$CF + M \rightarrow CF-M \quad (2c)$$

$$CH_3 + M \rightarrow CH_3-M \quad (2d)$$

$$CH_2(\text{notdetected}) + M \rightarrow CH_2-M, CH-MH \quad (2e)$$

However, the concentrations of the CH_3F fragments in the reaction medium are very low in comparison with that of CH_3F. For example, the concentration of the most abundant CH_2F estimated from the C−F stretching absorption intensities assuming the same extinction constants is $\sim 10^{-6}$ of that of CH_3F. The CF and CH_3 absorptions are also observed in the product spectra, but CF−M and previously reported CH_3-M[10] are not identified in this study. Moreover, no fluoromethyl metal (CH_2F-M) and its smaller fragments have been identified in the previous studies of transition-metal reactions with methyl fluoride.[11]

Thus, it is evidently more plausible that dissociation of the insertion complexes results in the smaller coinage metal complexes. The excess energy from insertion reaction or plume radiation would lead to H detachment from the Cu, Ag, and Au insertion complexes (292, 210, and 174 kJ/mol). The H-detachment energies of the F-containing complexes are higher than the 134, 110, and 137 kJ/mol for the previously observed corresponding methyl metal hydrides (CH_3-MH).[10] They are also compared with the H-detachment energies of 657, 325, and 277 kJ/mol estimated for CH_3-ZrF, CH_3-NiF, and CH_3-PtF. The dissociation energies of $CH_3-MF \rightarrow CF-MH + H_2$ for Cu, Ag, and Au are 369, 297, and 242 kJ/mol, and those of $CH_3-MF \rightarrow CH_2-M + HF$ are 162, 92, and 56 kJ/mol, respectively. The low dissociation energies of the gold insertion complex indicate that it is more prone to fragment to the smaller products than the Cu and Ag analogues, and the observed smaller Au complexes support the presumption that they originate from the insertion complex.

$$CH_3-MF^* \rightarrow CH_2F-M, CH_2-MF, \text{or } CHF-MH + H \quad (3a)$$

$$CH_3-MF^* \rightarrow CF-MH \text{ or } CHF-M + H_2 \quad (3b)$$

$$CH_3-MF^* \rightarrow CH_2-M + HF \quad (3c)$$

Unlike the previous studies of methane reactions with coinage metals, where the anionic insertion complexes are observed from the reactions with CH_4, no anionic species are observed in this study. It is shown that while the electron affinities of the group 11 metals are the highest among the transition metals,[32] those of the insertion complexes are even higher, probably due to stabilization of the negative charge by the methyl and hydride substituents.[10] Similarly, the anionic species are expected to be produced from the F-containing insertion complexes. The electron affinities of Cu, Ag, and Au are 119, 126, and 223 kJ/mol,[32] whereas those of CH_3-MF for Cu, Ag, and Au are 291, 331, and 370 kJ/mol. They are also compared with 226, 252, and 268 kJ/mol for coinage metal CH_3-MH species.

$$CH_3-MF + e^- \rightarrow CH_3-MF^- \quad (4)$$

However, the halogen-containing precursor is believed to serve as an electron scavenger as well, resembling the carbon tetrahalides (CX_4).[11,14] Due to the low free electron concentration in the reaction medium, the anionic species is most likely not produced in a sufficient amount to observe. It is also noticeable that only the CH_3 and M−F stretching bands of CH_3-MF^- are observably strong. The strongest CH_3 stretching bands of the anionic species are located in the congested region with the precursor C−H stretching absorptions while the M−F stretching frequencies are low (Tables S3, S6, and S13, Supporting Information), making them difficult to observe.

Structures of Small Au, Ag, and Cu Complexes. The structures of the group 11 metal complexes investigated in this study are illustrated in Figures 7−9. The C−M bond lengths of CH_3-MF and CH_3-MF^- are shorter than those of CH_3-MH and CH_3-MH^-, whereas that of CH_2F-M is longer than that of CH_3-M.[10] For example, the C−Cu bond lengths of 1.921, 1.935, and 1.935 Å for CH_3-CuF, CH_2F-Cu, and CH_3-CuF^- are compared with those of 1.963, 1.918, and 1.988 Å for CH_3-CuH, CH_3-Cu, and CH_3-CuH^-. Clearly, F bonded to M strengthens the C−M bond. As a result, the C−M bonds of CH_3-MF and CH_3-MF^- are shorter than or comparable with those of CH_2F-M, as shown in Figures 7−9. In contrast, the C−M bonds of CH_3-M for the coinage metals are much shorter than those of the insertion and anionic insertion complexes.[10] It is also noticeable that the C−Au bond length of CH_2-AuF (1.877 Å) is much shorter than those of CF−AuH (1.983 Å) and CH_3-AuF (2.046 Å). These values compare favorably with the sums of double and single bond covalent radii (188 and 199 pm) tabulated by Pyykkö et al.[33]

While the natural effective bond order[34] of CH_2F-M is still higher than CH_3-MF and CH_3-MF^- (Table S15, Supporting Information) parallel to the previously examined methyl metal species,[10] the natural C and M charges indicate that the C−M bonds of CH_3-MF and CH_3-MF^- are much more polarized than that of CH_2F-M. Without F substitution, the C−M bond order would be the single important factor in determining the bond strength. The higher ionic contributions to the C−M bonds of the insertion complexes apparently enhance their bond strength, resulting in C−M bond lengths smaller or comparable to that of CH_2F-M.

It is also interesting that the C−Au bonds of CF−AuH and CH_2-AuF contain substantial π character (bond orders of 1.271 and 1.869 (B3LYP) in Table S15, Supporting Information), and particularly the bond order of CH_2-AuF is near that for a true double bond. This methylidene complex is believed to be the first neutral gold compound evidenced by an experiment containing a C═Au double bond. On the other hand, the bond orders of CH_2-Au and CH_2-AuH are considerably lower (0.990 and 1.456), indicating that F lowers the 5d-orbital energy of Au for better overlap with the carbon 2p orbitals for π bonding. In order to test this hypothesis, CH_2-AuCl and CH_2-AuBr were calculated, and their C−Au double bond lengths are longer (1.904 and 1.912 Å) and their bond orders smaller (1.835 and 1.828, Table S15).

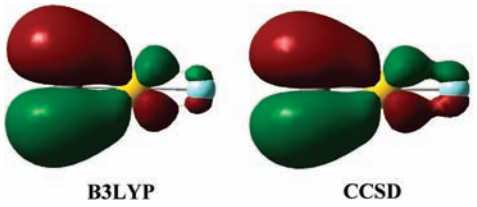

Figure 10. Bonding π molecular orbital for CH_2═AuF plotted using isodensity 0.02 $e^-/Å^3$.

The C−Au bond in singlet CH_2−AuF constitutes a σ bond [71.5% C using 37.7% s and 62.2% p and 28.5% Au using 76.3% s, 3.4% p, and 20.3% d] and a π bond [18.7% C as 100% p and 81.3% Au as 100% d] with the occupancies $(\sigma)^{2.00}(\pi)^{2.00}$-$(\pi^*)^{0.08}(\sigma^*)^{0.18}$ for an effective bond order of 1.869 (Table S15, Supporting Information),[34] which along with bond length matching the sum of covalent double bond radii of Pyykkö et al.,[33] supports the double bond description. The calculation with CCSD gives a similar 1.890 bond order. The bonding π molecular orbital for CH_2−AuF is shown in Figure 10. Figure 8 also shows an unusual, linear C−Ag−F moiety of CH_3−AgF, which is similar to the structures of the group 2 metal analogues[35] but contrasts bent structures of the small transition-metal insertion complexes.[11] Only the previous Mn and Fe analogues have shown linear C−M−X backbones.[36]

CONCLUSIONS

Reactions of laser-ablated group 11 metal atoms with CH_3F isotopomers have been carried out, and the products are identified from the matrix IR spectra on the basis of frequencies, isotopic shifts, and correlation with two DFT frequency calculations. The insertion complexes (CH_3−MF) are identified along with fluoromethyl metal complexes (CH_2F−M), whereas no anionic insertion complexes are observed, unlike the previous results for group 11 metal reactions with methane.[10] Following the previously examined reactions with CH_4, the coinage metals readily undergo C−F bond insertion and H detachment to form the insertion and fluoromethyl complexes. In addition, smaller gold complexes (CF−AuH, CH_2−Au, and CH_2−AuF) are also observed in the Au + CH_3F spectra.

While the reaction medium contains the CH_3F fragments, the fluoromethyl coinage metals (CH_2F−M) and smaller gold complexes probably originate from dissociation of the insertion complexes, because some of the expected fragments such as CH_3M are not observed and the analogues in other transition-metal systems have not been observed. The small gold complexes observed are in line with the relatively small dissociation energies of CH_3−AuF to form them. The C−M bonds of CH_3−MF and CH_3−MF^- are shorter than those of CH_3−MH and CH_3−MH^-, whereas that of CH_2F−M is longer than that of CH_3−M, making the C−M bonds of the insertion complexes smaller or comparable to that of CH_2F−M. F bonded to the M center increases polarization of the C−M bond, and this ionic contribution strengthens the bond. NBO analyses show that the C−Au bonds of CF−AuH and CH_2−AuF possess considerable π character, and CH_2−AuF incorporates a true double bond. In contrast, the bond orders of CH_2−Au, CH_2−AuH, and CH_2−AuCl are lower, indicating that F bonded to Au reduces the 5d-orbital energy for better overlap with the carbon 2p orbital for π-bonding.

ASSOCIATED CONTENT

Supporting Information. Tables S1−S15 of calculated frequencies and NBO results. Figures S1−S3 of infrared spectra from experiments using $^{13}CH_3F$. This material is available free of charge via the Internet at http://pubs.acs.org.

AUTHOR INFORMATION

Corresponding Author
*E-mail: lsa@virginia.edu.

ACKNOWLEDGMENT

We gratefully acknowledge financial support from the National Science Foundation (U.S.), Grant CHE 03-52487 to L.A., and support from the Korea Research Foundation (KRF), grant funded by the Korean government (MEST; No. 2009-0075428).

REFERENCES

(1) Au reviews: (a) Schmidbaur, H.; Schier, A. *Organometallics* **2010**, *29*, 2. (b) Gorin, D. J.; Sherry, B. D.; Toste, F. D. *Chem. Rev.* **2008**, *108*, 3351. (c) Arcadi, A. *Chem. Rev.* **2008**, *108*, 3266. (d) Jiménez-Núñez, E.; Echavarren, A. M. *Chem. Rev.* **2008**, *108*, 3326. (e) Li, Z.; Brouwer, C.; He, C. *Chem. Rev.* **2008**, *108*, 3239. (f) Pyykkö, P. *Angew. Chem., Int. Ed.* **2004**, *43*, 4412. Pyykkö, P. *Chem. Soc. Rev.* **2008**, *37*, 1967. Au catalysis: (g) Haruta, M.; Yamada, N.; Kobayashi, T.; Iijima, S. *J. Catal.* **1989**, *115*, 301.

(2) Ag reviews: (a) Weibel, J.-M.; Blanc, A.; Pale, P. *Chem. Rev.* **2008**, *108*, 3149. (b) Tyrra, W. *Heteroatom Chem.* **2002**, *13*, 561.

(3) Cu reviews: (a) Breit, B.; Schmidt, Y. *Chem. Rev.* **2008**, *108*, 2928. (b) Caprio, V. *Lett. Org. Chem.* **2006**, *3*, 339.

(4) SERS reviews: (a) Pastoriza-Santos, I.; Alvarez-Puelbla, R. A.; Liz-Marzán, L. M. *Eur. J. Inorg. Chem.* **2010**, 4288. (b) Casadio, F.; Leona, M.; Lombardi, J. R.; Duyne, R. V. *Acc. Chem. Res.* **2010**, *43*, 782. (c) Porter, M. D.; Lipert, R. J.; Siperko, L. M.; Wang, G.; Narayanan, R. *Chem. Soc. Rev.* **2008**, *37*, 1001.

(5) CH_3-Ag: (a) O'Hair, R. A. J. *Chem. Commun.* **2002**, 20. (b) Rabinovitch, B. S.; Dills, D. H.; Larson, N. R. *J. Phys. Chem.* **1959**, *63*, 1523. (c) Semerano, G.; Riccoboni, L. *Ber. Deutsch. Ges. B* **1941**, *74B*, 1089.

(6) CH_3-Cu: (a) Grotjahn, D. B.; Halfen, D. T.; Ziurys, L. M.; Cooksy, A. L. *J. Am. Chem. Soc.* **2004**, *126*, 12621. (b) Nakamura, E.; Mori, S.; Nakamura, M.; Morokuma, K. *J. Am. Chem. Soc.* **1997**, *119*, 4887. (c) Gilman, H.; Jones, R. G.; Woods, L. A. *J. Org. Chem.* **1952**, *17*, 1630.

(7) (a) Parnis, J. M.; Mitchell, S. A.; Garcia-Prieto, J.; Ozin, G. A. *J. Am. Chem. Soc.* **1985**, *107*, 8169. See also:(b) Billups, W. E.; Konarski, M. M.; Hauge, R. H.; Margrave, J. L. *J. Am. Chem. Soc.* **1980**, *102*, 7393. (c) Ritter, D.; Carroll, J. J.; Weisshaar, J. C. *J. Phys. Chem.* **1992**, *96*, 10636.

(8) CH_3-AgH^- and CH_3-CuH^-: (a) Rijs, N. J.; O'Hair, R. A. J. *Organometallics* **2010**, *29*, 2282. (b) Rijs, N. J.; O'Hair, R. A. *Organometallics* **2009**, *28*, 2684.

(9) Chang, S.-C.; Kafafi, Z. H.; Hauge, R. H.; Billups, W. E.; Margrave, J. L. *J. Am. Chem. Soc.* **1987**, *109*, 4508.

(10) Cho, H.-G.; Andrews, L. *Dalton Trans.* **2011**, *40*, [Online] DOI:10.1039.10.1039/C0DT01827A.

(11) (a) Andrews, L.; Cho, H.-G. *Organometallics* **2006**, *25*, 4040 and references therein. (b) Cho, H.-G.; Andrews, L. *Dalton Trans.* **2010**, *39*, 5478. (c) Cho, H.-G.; Andrews, L. *J. Am. Chem. Soc.* **2008**, *130*, 15836. (d) Cho, H.-G.; Andrews, L. *J. Am. Chem. Soc.* **2004**, *126*, 10485. (e) Cho, H.-G.; Andrews, L. *Organometallics* **2009**, *28*, 1358.

(12) CH_3-CuF, ESR: Knight, L. B., Jr.; Cobranchi, S. T.; Gregory, B. W.; Jones, G. C., Jr. *J. Chem. Phys.* **1988**, *88*, 524.

(13) $M^+ + CH_3F$: (a) Zhao, X. Z.; Koyanagi, G. K.; Bohme, D. K. *J. Phys. Chem. A* **2006**, *110*, 10607. $AuCH_2^+$: (b) Li, F.-X.; Armentrout, P. B. *J. Chem. Phys.* **2006**, *125*, 133114.

(14) (a) Andrews, L.; Citra, A. *Chem. Rev.* **2002**, *102*, 885 and references therein. (b) Andrews, L. *Chem. Soc. Rev.* **2004**, *33*, 123 and references therein.

(15) (a) von Frantzius, G.; Streubel, R.; Brandhorst, K.; Grunenberg, J. *Organometallics* **2006**, *25*, 118 and references therein. (b) Berkaine, N.; Reinhardt, P.; Alikhani, M. E. *Chem. Phys.* **2008**, *343*, 241. (c) Chung, G.; Gordon, M. S. *Organometallics* **2003**, *22*, 42. (d) de Jong, G. T.; Bickelhaupt, F. M. *J. Chem. Theory Comput.* **2007**, *3*, 514. (e) Roos, B. O.; Lindh, R.; Cho, H.-G.; Andrews, L. *J. Phys. Chem. A* **2007**, *111*, 6420.

(16) Frisch, M. J.; Trucks, G. W.; Schlegel, H. B.; Scuseria, G. E.; Robb, M. A.; Cheeseman, J. R.; Scalmani, G.; Barone, V.; Mennucci, B.; Petersson, G. A.; Nakatsuji, H.; Caricato, M.; Li, X.; Hratchian, H. P.; Izmaylov, A. F.; Bloino, J.; Zheng, G.; Sonnenberg, J. L.; Hada, M.; Ehara, M.; Toyota, K.; Fukuda, R.; Hasegawa, J.; Ishida, M.; Nakajima, T.; Honda, Y.; Kitao, O.; Nakai, H.; Vreven, T.; Montgomery, J. A., Jr.; Peralta, J. E.; Ogliaro, F.; Bearpark, M.; Heyd, J. J.; Brothers, E.; Kudin, K. N.; Staroverov, V. N.; Kobayashi, R.; Normand, J.; Raghavachari, K.; Rendell, A.; Burant, J. C.; Iyengar, S. S.; Tomasi, J.; Cossi, M.; Rega, N.; Millam, N. J.; Klene, M.; Knox, J. E.; Cross, J. B.; Bakken, V.; Adamo, C.; Jaramillo, J.; Gomperts, R.; Stratmann, R. E.; Yazyev, O.; Austin, A. J.; Cammi, R.; Pomelli, C.; Ochterski, J. W.; Martin, R. L.; Morokuma, K.; Zakrzewski, V. G.; Voth, G. A.; Salvador, P.; Dannenberg, J. J.; Dapprich, S.; Daniels, A. D.; Farkas, Ö.; Foresman, J. B.; Ortiz, J. V.; Cioslowski, J.; Fox, D. J. *Gaussian 09*, Revision B.01; Gaussian, Inc.: Wallingford, CT, 2010.

(17) (a) Becke, A. D. *J. Chem. Phys.* **1993**, *98*, 5648. (b) Lee, C.; Yang, Y.; Parr, R. G. *Phys. Rev. B* **1988**, *37*, 785.

(18) Raghavachari, K.; Trucks, G. W. *J. Chem. Phys.* **1989**, *91*, 1062.

(19) Andrae, D.; Haeussermann, U.; Dolg, M.; Stoll, H.; Preuss, H. *Theor. Chim. Acta* **1990**, *77*, 123.

(20) (a) Becke, A. D. *Phys. Rev. A* **1988**, *38*, 3098. (b) Burke, K.; Perdew, J. P.; Wang, Y. In *Electronic Density Functional Theory: Recent Progress and New Directions*; Dobson, J. F., Vignale, G., Das, M. P., Ed.; Plenum: Berlin, 1998.

(21) (a) Scott, A. P.; Radom, L. *J. Phys. Chem.* **1996**, *100*, 16502. (b) Andersson, M. P.; Uvdal, P. L. *J. Phys. Chem. A* **2005**, *109*, 2937.

(22) Jacox, M. E. *J. Phys. Chem. Ref. Data* **1994**, *Monograph 3*, 1. **1998**, *27* (2), 115. **2003**, *32* (1), 1.

(23) Au, Ag, Cu + H_2: (a) Andrews, L.; Wang, X. *J. Am. Chem. Soc.* **2003**, *125*, 11751. (b) Wang, X.; Andrews, L.; Manceron, L.; Marsden, C. *J. Phys. Chem. A* **2003**, *107*, 8492.

(24) Wang, X.; Andrews, L. Unpublished data.

(25) Moore, C. E. Atomic Energy Levels. *Circular of the US Nat'l. Bur. Stds. 467*; U.S. National Bureau of Standards: Washington, DC, 1958

(26) (a) Evans, C. J.; Lesarri, A.; Gerry, M. C. L. *J. Am. Chem. Soc.* **2000**, *122*, 6100. (b) Thomas, J. M.; Walker, N. R.; Cooke, S. A.; Gerry, M. C. L. *J. Am. Chem. Soc.* **2004**, *126*, 1235. (c) Evans, C. J.; Rubinoff, D. J.; Gerry, M. C. L. *Phys. Chem. Chem. Phys.* **2000**, *2*, 3943.

(27) (a) Belpassi, L.; Infante, I.; Tarantelli, F.; Visscher, L. *J. Am. Chem. Soc.* **2008**, *130*, 1048. (b) Evans, C. J.; Wright, T. G.; Gardner, A. M. *J. Phys. Chem. A* **2010**, *114*, 4446.

(28) Pyykkö, P. *Chem. Rev.* **1988**, *88*, 563 and references therein.

(29) Pople, J. A.; Krishnan, R.; Schlegel, H. B.; Binkley, J. S. *Int. J. Quantum Chem.* **1978**, *14*, 545.

(30) (a) Cho, H.-G.; Andrews, L. *Dalton Trans.* **2009**, 5858. (b) Cho, H.-G.; Andrews, L. *Inorg. Chem.* **2007**, *46*, 8728. (c) Lyon, J. T.; Cho, H.-G.; Andrews, L. *Organometallics* **2007**, *26*, 6373.

(31) (a) Milligan, D. E.; Jacox, M. *J. Chem. Phys.* **1967**, *47*, 5146. (b) Jacox, M. E.; Milligan, D. E. *J. Chem. Phys.* **1969**, *50*, 3252. (c) Andrews, L. *J. Phys. Chem.* **1984**, *88*, 2940. (d) Raymond, J. I.; Andrews, L. *J. Phys. Chem.* **1971**, *75*, 3235.

(32) (a) Pauling, L. *J. Am. Chem. Soc.* **1932**, *54*, 3570. (b) For an updated comparison, see: http://en.wikipedia.org/wiki/Electron_affinity (accessed Sep 2011).

(33) Triple bond radii: (a) Pyykkö, P; Riedel, S.; Patzschke, M. *Chem.—Eur. J.* **2005**, *12*, 3511. Double bond radii: (b) Pyykkö, P.; Atsumi, M. *Chem.—Eur. J.* **2009**, *15*, 12770. Single bond radii: (c) Pyykkö, P.; Atsumi, M. *Chem.—Eur. J.* **2009**, *15*, 186.

(34) Reed, A. E.; Curtiss, L. A.; Weinhold, F. *Chem. Rev.* **1988**, *88*, 899 and references therein.

(35) Grignard reagent: (a) Kauffmann, T.; Bisling, M. *Tetrahedron Lett.* **1984**, *25*, 293. (b) Cahiez, G.; Alami, M. *Tetrahedron Lett.* **1986**, *27*, 569.

(36) (a) Cho, H.-G.; Andrews, L. *Organometallics* **2011**, *30*, 477. (b) Cho, H.-G.; Andrews, L. *J. Phys. Chem. A* **2011**, *115*, 4929. (c) Cho, H.-G.; Lyon, J. T.; Andrews, L. *Organometallics* **2008**, *27*, 5241.